A Dynamic Model for Induced Reactivation of Latent Virus

G.M. Kepler[1,5], H.K. Nguyen[2,5], J. Webster-Cyriaque[3,6], and H.T. Banks[4,5]

[5] Center for Research in Scientific Computation
North Carolina State University
Raleigh, N.C. 27695-8205, USA

[6] Department of Dental Ecology
School of Dentistry
University of North Carolina
Chapel Hill, N.C., USA

December 4, 2005

Send correspondence and reprint requests to:
G.M. Kepler
Center For Research in Scientific Computation
Box 8205 North Carolina State University
Raleigh, NC 27695-8205
Telephone, 919-515-8966; Fax, 919-515-8967

Abstract

We develop a deterministic mathematical model to describe reactivation of latent virus by chemical inducers. This model is applied to the reactivation of latent KSHV in BCBL-1 cell cultures with butyrate as the inducing agent. Parameters for the model are first estimated from known properties of the exponentially growing, uninduced cell cultures. The model is then extended to describe chemically induced KSHV reactivation in latently infected BCBL-1 cells. Additional parameters that are necessary to describe induction are determined from fits to experimental data from the literature. Our model provides good agreement with two independent sets of experimental data.

[1]email: gmkepler@ncsu.edu
[2]email: hknguyen@ncsu.edu
[3]email: cyriaquj@dentistry.unc.edu
[4]email: htbanks@ncsu.edu

1 Introduction

Many viral pathogens establish latency and are dormant. The presence of inducers leads these pathogens to reactivate and replicate, aiding their transmission and contributing to disease development. In addition, there is increasing evidence in the literature for the importance of polymicrobial infections in which microorganisms interact in a synergistic fashion, impacting both pathogenesis and maintenance of health. Among these, virus-bacteria interactions have been described, including reactivation of latent virus by metabolic end products of anaerobic bacteria. A shift in the balance of the flora often controlled by the intact immune system may reflect significant morbidity particularly in the immune suppressed host. The relationships between viral pathogens and their inducing agents have not previously been described mathematically. Therefore, to begin to understand the relationship between pathogens and their inducing agents, particulary in a polymicrobial environment, we have developed a mathematical model that describes the reactivation of latent herpes virus by metabolic end products of anaerobic bacteria.

Herpes viruses are double-stranded DNA viruses. Currently, there are eight known herpes viruses that infect humans. After primary infection, the virus remains latent in specific types of host cells that may be different from the types of cells targeted for primary infection. Latent virus persists in the cell nucleus as episomal DNA until it is reactivated, beginning a program of lytic replication and lysis, and leading to a new (sometimes asymptomatic) round of infection and latency. Upon the reactivation, the viral DNA begins a lytic program characterized by a temporal cascade of gene expression culminating in excretion of free virus and cell lysis. The lytic program is typically described as three phases of gene expression: Immediate Early, Early, and Late. During Immediate Early and Early phases infected cells produce viral proteins that are necessary for viral DNA synthesis, which occurs at the end of the Early phase. During the Late phase of the reproductive cycle the host cell is directed to make the structural proteins necessary for viral packaging.

The exact mechanisms by which latent virus becomes reactivated and begins lytic replication are not entirely known. However, it has been established that inducing agents such as Tetradecanoyl Phorbol Acetate (TPA), sodium butyrate, and other short chain fatty acids (SFAs) can induce lytic replication of Kaposi's Sarcoma-associated Herpes virus (KSHV) and Epstein-Barr virus (EBV) [14, 37, 38]. In addition, recent experiments have shown that the spent media from gram negative bacteria cultures, such as P. Gingivalis and P. Intermedia, which contains short chain fatty acids (e.g., iso-valeric, n-butyric acid, and propionic acid), can also induce latent KSHV to begin lytic replication [29].

A mechanism for bacterial reactivation of latently infected cells has strong health implications for the oral environment as well as the gut and GI tract, where there may be large numbers of gram negative bacteria in the presence of latently-infected cells. Reactivation of latent herpes viruses are a major health concern for immune-compromised individuals, such as those with AIDS. Understanding the role of anaerobic bacteria in reactivation of latent herpes viruses may have important health consequences if there is similar reactivation of latent episomal HIV by bacterial metabolic end products.

To our knowledge there has been no mathematical modeling treatment of viral reactivation at the cellular level. Much of the mathematical modeling of herpes viruses has focused, understandably, on modeling at the epidemiological level (*e.g.*, [7, 18]). Recently, Wang *et al.,* used HHV-6 infection as a stimulus for studying cellular changes in the T cell immune system under pathological conditions [34]. Their study included data from the literature, clinical data, and cell culture data. Their model agreed well with data, but focused on the viral load and T cell response. Clearly there is a need and opportunity to understand viral latency and reactivation, especially since this is a characteristic feature of herpes virus infection.

In this manuscript we report on a deterministic mathematical model that we have developed to describe reactivation of latent virus by chemical inducers. In particular, we apply this model to the reactivation of latent KSHV in BCBL-1 cell cultures with butyrate as the inducing agent. KSHV, also known as Human Herpesvirus-8 (HHV-8), is a gamma herpes virus that is responsible for Kaposi's Sarcoma tumor development and other lymphoproliferative disorders such as Castleman's disease and primary effusion lymphoma. KSHV latently infects epithelial and lymphoid cells that are present in the oral environment and reactivation of latent virus in B cells may play a role in the pathogenesis of Kaposi's sarcoma [25]. BCBL-1 cells are an

immortalized cell line derived from body-cavity-based lymphomas that are latently infected with multiple copies of KSHV, but not Epstein-Barr virus (EBV) [28], providing a convenient vehicle for studies of viral reactivation. We choose butyrate as the inducing agent since, as an SFA, it is similar to the metabolic end products of gram negative bacteria, it is easily quantified, and its activity is well documented in the experimental literature.

We first estimate parameters for our model from known properties of the exponentially growing, uninduced cell cultures. We then extend the model to describe chemically induced KSHV reactivation in latently infected BCBL-1 cells. Additional parameters that describe induction are determined from fits to experimental data available in the literature. Our model exhibits good agreement with two independent sets of experimental data.

The model presented here establishes a general framework for modeling the effect of other inducing agents that act through histone-deacetylase (HDAC) inhibition, including other SFA's produced by the metabolic processes of gram negative bacteria. As such, it may also be applied to other latent virus systems that are induced to replicate via HDAC inhibition, such as EBV, HIV, and HCMV.

2 Modeling Compartments

We describe the dynamics of the host cells and viral DNA copies using a set of ordinary differential equations (ODEs). A schematic diagram of the ODE model compartments is shown in Figure 1 and the model compartments are summarized in Table 1. Latent L and lytic R copies of viral DNA reside in the nuclei of host cells. As mentioned above, there are multiple copies of episomal viral DNA in each BCBL-1 host cell. We make the following "all or nothing" simplifying assumption: within a given host cell, nuclear viral DNA copies are either all latent or all in a lytic replication program. Therefore, there are two types of host cells, host cells H_R with lytic virus only or host cells H_L with latent virus only. In future work, we may superimpose a probability distribution on the parameters to better approximate mixed conditions where a host cell may contain both latent and lytic virus in varying levels. Such a modeling technique was successfully used in cellular level HIV models to account for variable length (with uncertainty) pathways in [2]. In models of this type the state variables are the *expected values* of concentrations (or of numbers of cells) resulting in delay differential equation models embodying uncertainty. We do not pursue this level of refinement in the initial model developed here.

Host cell death can occur as a result of natural aging, with individual rates d_R and d_L, viral lysis rate d_I [30], or the inducing agent rates $\delta_L(s)$ and $\delta_R(s)$. Host cells that die are added to a nonviable host cell compartment N. During the Early Phase of the lytic program, productive replication of viral DNA takes place in replication compartments [35]. The localization of the replication process allows for exponential-like growth of viral DNA R, where the progeny of replicating virus become replication templates themselves [16]. Capsid assembly occurs in the nucleus and nucleocapsid envelopment occurs at the nuclear membrane. The intracellular viral DNA compartment V_I represents viral DNA copies that are no longer targets for replication and are available for encapsulation.

After envelopment, the virus is released as free virions V_F. Experiments by Bechtel *et al.,* indicate that free KSHV virions produced by BCBL-1 cells fail to infect many cultured lymphoid cell lines [5]. Therefore, we assume that free virions that are produced are not capable of reinfecting the host cells. We can also arrive at this assumption by considering that, within the cultured cell line, there are always a small number of host cells with spontaneously reactivated lytic virus that are producing free virions. If the free virus were able to reinfect the BCBL-1 cells then the average number of viral copies per host cell would not be a stable quantity. Since there is no indication that the average number of viral DNA copies in the cell line is changing with time, we assume that free virions are not reinfecting the host cells.

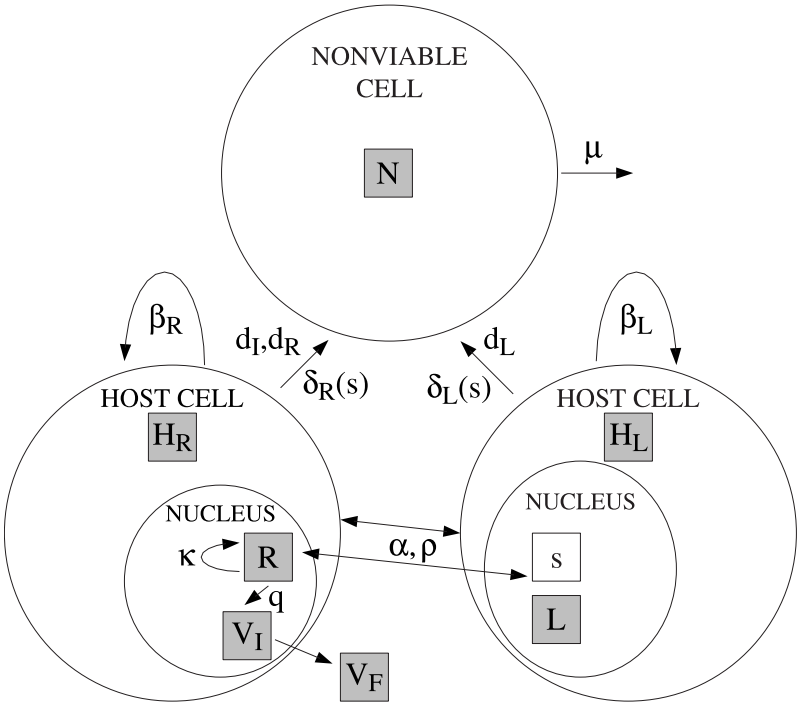

Figure 1: Schematic of the modeling compartments associated with latent virus host cells H_L, lytic virus host cells H_R, and nonviable host cells N. Latent virus L reactivates to become lytic virus R, either spontaneously or in response to an inducing agent s. Lytic virus R undergoes exponential growth until it passes to the intracellular viral compartment V_I where it is available for packaging and is released as free virions V_F.

Compartment	Symbol	Units
Host cells (latent virus only)	H_L	number of cells
Host cells (lytic virus only)	H_R	number of cells
Nonviable cells	N	number of cells
Latent virus	L	DNA copies
Lytic Virus	R	DNA copies
Intracellular virus	V_I	DNA copies
Free virus	V_F	number of virions

Table 1: ODE Model Compartments.

3 Mathematical Model for the Uninduced Case

Host cell dynamics. Latently infected host cells H_L are growing at a rate $\beta_L H_L$ and have a natural death rate $d_L H_L$, where $\beta_L > d_L$. As part of the lytic cycle, herpes viruses block the cell cycle in G_0/G_1 and block cell-initiated apoptosis [17, 20, 36]. Therefore, host cells with lytic virus H_R are expected to have much smaller rates of cell replication $\beta_R H_R$ and natural death $d_R H_R$ than host cells with latent virus ($\beta_R \ll \beta_L$ and $d_R \ll d_L$). Although lytically infected host cells H_R are expected to have a reduced death rate due to viral inhibition of apoptosis, there is an additional mechanism for cell death due to the production of virus and the resulting cell lysis. We model this viral-induced death rate as a function of the average amount of intracellular virus that accumulates $d_I(\bar{V}_I)H_R$, where $\bar{V}_I = V_I/H_R$. Nonviable cells are in a process of

disintegration into smaller fragments and leave the N compartment with a rate μN.

Experimental observations of uninduced cell cultures indicate that some fraction of host cells will, through spontaneous reactivation, have lytic virus [8, 23, 27]. Therefore, we include terms for spontaneous reactivation of latently infected cells with a rate constant α_0. When herpes viruses establish latency in newly infected cells they undergo a small lytic replication program using proteins imported in the viral capsid. Rather than proceeding to encapsulation and lysis, the replicated copies of viral DNA then enter a latent state [16]. This initial lytic infection that leads to latency is different from the lytic replication that occurs when latent virus in cultured cells is induced into a lytic program and it is not clear whether virus that is reactivated from latency can return to a latent state in these cultured cells. Therefore, we allow for the possibility that lytic virus returns to a latent state with a rate ρR. Later we will present an argument that this term must be zero in a cell culture with a stable average viral copy number. With these considerations in mind, we model the host cell dynamics in the uninduced case by

$$\begin{aligned}
\frac{dH_L}{dt} &= (\gamma_L - \alpha_0)\, H_L + \rho H_R \\
\frac{dH_R}{dt} &= \alpha_0 H_L + \left(\gamma_R - \rho - d_I(\bar{V}_I)\right) H_R \\
\frac{dN}{dt} &= d_L H_L + \left(d_R + d_I(\bar{V}_I)\right) H_R - \mu N\,,
\end{aligned} \tag{3.1}$$

where $\gamma_L = \beta_L - d_L$ and $\gamma_R = \beta_R - d_R$.

Viral dynamics. There are multiple copies of viral DNA in each latently infected host cell nucleus, with an average $\bar{L}$ per cell. Latent virus is maintained as circular episomal DNA in the host cell nucleus where it is tethered to the host cell DNA and is copied each time the host cell DNA is replicated. Therefore we can approximate the L compartment growth at a rate which is proportional to the host cell growth rate and the average number of latent virus copies per host cell, $\bar{L}\beta_L H_L$. We allow for the possibility that lytic virus R is also copied during host cell replication, although as stated above, we expect the host cells with lytic virus to be replicating at a much lower rate. This gives a similar growth rate of $\bar{R}\beta_R H_R$ for lytic virus.

Using the same reasoning, we assume that each dying host cell destroys a number of latent (lytic) virus equal to the average number of latent (lytic) virus per host cell, as represented by the loss term $\bar{L}d_L H_L$ ($\bar{R}d_R H_R$ and $\bar{R}d_I(\bar{V}_I)H_R$). We assume that the intracellular viral DNA copies are not replicated with the host cell, since they are not tethered to the host DNA, but are destroyed when the host cell dies at rates of $\bar{V}_I d_I(\bar{V}_I)H_R$ and $\bar{V}_I d_R H_R$. The reactivation and deactivation of latent and lytic virus follows in a manner similar to the terms above. Therefore, the uninduced model for the viral DNA dynamics is given by the set of equations

$$\begin{aligned}
\frac{dL}{dt} &= \gamma_L \bar{L} H_L - \alpha_0 \bar{L} H_L + \rho \bar{R} H_R \\
\frac{dR}{dt} &= (\kappa - q)R + \alpha_0 \bar{L} H_L + \left(\gamma_R - d_I(\bar{V}_I)\right) H_R \bar{R} - \rho H_R \bar{R} \\
\frac{dV_I}{dt} &= qR - pV_I - d_R H_R \bar{V}_I - d_I(\bar{V}_I) H_R \bar{V}_I \\
\frac{dV_F}{dt} &= pV_I,
\end{aligned} \tag{3.2}$$

where κR is the replication rate for lytic viral DNA, qR is the rate at which lytic virus moves to the intracellular compartment, and pV_I is the rate at which the intracellular DNA is packaged and excreted as free virions V_F.

Uninduced cell and viral dynamics. Using $\bar{L} = L/H_L$, $\bar{R} = R/H_R$ and $\bar{V}_I = V_I/H_R$, we can write the full uninduced model as

$$\begin{aligned}
\frac{dH_L}{dt} &= (\gamma_L - \alpha_0)H_L + \rho H_R \\
\frac{dH_R}{dt} &= \alpha_0 H_L + \left(\gamma_R - d_I(\bar{V}_I) - \rho\right) H_R \\
\frac{dN}{dt} &= d_L H_L + \left(d_R + d_I(\bar{V}_I)\right) H_R - \mu N \\
\frac{dL}{dt} &= (\gamma_L - \alpha_0)L + \rho R \\
\frac{dR}{dt} &= \left(\kappa - q + \gamma_R - d_I(\bar{V}_I) - \rho\right) R + \alpha_0 L \\
\frac{dV_I}{dt} &= qR - \left(p + d_R + d_I(\bar{V}_I)\right) V_I.
\end{aligned} \tag{3.3}$$

The solution for V_F is easily obtained from the above solutions and can be written as

$$V_F(t) = V_{F0} + \int_{t_0}^{t} pV_I(u)du. \tag{3.4}$$

4 Mathematical Model for the Induced Case

We next modify the uninduced model (3.3) to include the actions of an inducing agent s. The main affect of the inducing agent is to increase the rate at which latent virus becomes reactivated ($\alpha(s) \geq \alpha_0$). In addition, inducing agents such as butyrate and valproate may also cause host cell death through activation of host cell genes [6, 22, 37]. We represent the induced cell death rates by $\delta_R(s)H_R$ and $\delta_L(s)H_L$, where $\delta_L(s)$ and $\delta_R(s)$ are functions of the butyrate concentration s. With these additional terms the equations for the induced case become

$$\begin{aligned}
\frac{dH_L}{dt} &= \left(\gamma_L - \alpha(s) - \delta_L(s)\right) H_L + \rho H_R \\
\frac{dH_R}{dt} &= \left(\gamma_R - \delta_R(s) - d_I(\bar{V}_I)\right) H_R + \alpha(s) H_L - \rho H_R \\
\frac{dN}{dt} &= \left(d_L + \delta_L(s)\right)H_L + \left(d_R + \delta_R(s) + d_I(\bar{V}_I)\right) H_R \\
\frac{dL}{dt} &= \left(\gamma_L - \alpha(s) - \delta_L(s)\right) L + \rho R \\
\frac{dR}{dt} &= \left(\kappa - q + \gamma_R - \delta_R(s) - d_I(\bar{V}_I)\right) R + \alpha(s) L - \rho R \\
\frac{dV_I}{dt} &= qR - \left(p + d_R + d_I(\bar{V}_I) + \delta_R(s)\right) V_I
\end{aligned} \tag{4.5}$$

and

$$V_F(t) = V_{F0} + \int_{t_0}^{t} pV_I(u)du. \tag{4.6}$$

5 Parameter Estimation

Some of the parameters in the uninduced model (3.3) can be estimated from physiological considerations. The parameter q is the rate constant for movement of lytically replicating virus from the R compartment to the intracellular compartment V_I. We estimate that the rate at which lytic virus leaves the R compartment is inversely proportional to the time that the lytic virus spends in the lytic program of gene expression and replication. Therefore, we set $q = 1/T$, where T is the approximate time it takes to complete the lytic program (approximately 48 hours).

Since the lytic virus causes cell cycle arrest and inhibits apoptosis, we make the simplifying assumptions that, for lytically infected host cells H_R, the growth rate constant and natural death rate constant both vanish, i.e., $\gamma_R = d_R = 0$. Although lytically infected host cells H_R are expected to have a reduced rate of death due to viral inhibition of apoptosis, there is an additional mechanism for cell death due to the production of virus and the resulting cell lysis. We have modeled the rate for this viral-induced death as a function of the average amount of intracellular virus that accumulates which is denoted by $d_I(\bar{V}_I)$, where $\bar{V}_I = V_I/H_R$. For the sake of simplicity and in the interest of obtaining parameter estimates, we assume d_I to be a linear function of the average number of intracellular copies per lytically infected host cell, i.e., $d_I(\bar{V}_I) = c\bar{V}_I$.

Implications of the ρ term on cell culture stability. We expect that the average number of latent copies of viral DNA per latently infected host cell is a constant that is characteristic of the particular cell line; otherwise the cell properties would be different from one experiment to the next. Therefore, $L/H_L = \bar{L}$ is a constant, which we designate with the variable n, and $dL/dt = n(dH_L/dt)$. Using these conditions and the first and fourth equations in (3.3), we find that $\rho(R - nH_R) = 0$. This condition can be met in two ways, either $\rho = 0$ or $R = nH_R$. The former condition requires that there is no reversion of lytically infected host cells back to latency. The latter condition implies that $dR/dt = n(dH_R/dt)$ and, from the second and fifth equations in (3.3), this condition would require that $\kappa - q = 0$. Since κR is the rate of replication of lytic virus and qR is the rate at which the lytic virus is moving to the intracellular virus compartment, the condition $\kappa - q = 0$ implies that there can be no net accumulation of replicating virus. If $\kappa - q = 0$ there will be no exponential growth of viral DNA copies. Such a condition is contrary to current knowledge of the lytic cycle for KSHV [16].

In summary, if the condition $\bar{L} = n$ is to be maintained in the uninduced BCBL-1 cell cultures then either there can be no reversion of virus back to latency ($\rho = 0$) or the rate at which the lytic viral DNA is being copied must be equal to the rate at which viral DNA copies are being added to the V_I compartment ($\kappa - q = 0$). The latter condition implies that copies of replicated viral DNA can not be templates for replication, themselves, which contradicts the current understanding of the lytic replication. Therefore, we set $\rho = 0$ in this model. It should be noted that these conditions only apply in the case of stable, latently infected cell lines such as BCBL-1 cells and do not apply to acutely infected cells where lytic virus is known to revert to latency.

Properties of cell lines. Other parameters in the uninduced model (3.3) can be estimated from known properties of the uninduced cell cultures. As we have noted, BCBL-1 cells are an immortalized cell line derived from body-cavity-based lymphomas that are latently infected with multiple copies of KSHV [28]. Exponentially growing cells are maintained in a medium consisting of growth nutrients and antibiotics to prevent bacterial contamination. Growing cells are periodically split to prevent contact growth inhibition and to provide fresh nutrients. We expect that, under constant growth and maintenance conditions, certain average properties of the cell line will be unchanging in time. Some of the parameters for the uninduced model can be estimated from these constants.

Table 2 summarizes these constants, along with ranges of values reported in the experimental literature. One such constant is the fraction of host cells with spontaneously reactivated virus a_s. Experimental observations of this quantity vary from 1-8%. Differences in observed values for a_s may be due to the different methods used to detect lytic virus as well as differences in the growth and maintenance conditions of the cell lines. Another constant is the fraction of nonviable cells N_r in the cell culture, with values reported from 8-20%. Variability in the observed fraction of nonviable cells N_r is, also, most likely a result of differences in cell

line growth and maintenance conditions as well as differences in measurement techniques (*e.g.*, dye exclusion versus dye inclusion identification techniques and haemocytometer versus cell sorting counting techniques). BCBL-1 cells have a doubling time D_p of approximately 48 to 85 hours, which will also be dependent upon growth and maintenance conditions. The model parameter n, which represents the average number of latent virus copies per uninduced host cell is a constant of the cell line, independent of growth and maintenance conditions. This quantity is not measured directly, but rather a related quantity n_T, representing the average number of copies of viral DNA per cell (or average cell-associated viral DNA, i.e., $L+R+V_I$), is measured. Values of n_T ranging from 50 to 70, dependent upon growth and maintenance conditions, have been reported in the literature.

In Table 2 the uninduced cell line constants are specified in terms of the ODE model compartments. The subscript $t \to \infty$ indicates that we expect these quantities to be constants in an equilibrated average sense under conditions of constant growth and maintenance. In addition to the above observed cell line constants, we also expect that the average number of lytic R_A and intracellular V_{IA} DNA copies per host cell to be constant though we have no experimental measurements for these constants.

Constant Description	Symbol	Value	Units	Model Formulation
Fraction of lytic host cells [13, 26, 33]	a_s	0.01-0.08	-	$a_s = \left(\frac{H_R}{H_L+H_R+N}\right)_{t\to\infty}$
Fraction of nonviable host cells [37, 38]	N_r	0.08-0.2	-	$N_r = \left(\frac{N}{H_L+H_R+N}\right)_{t\to\infty}$
Host cell doubling time [24, 33]	D_p	48-85	hr	$2 = \frac{(H_L+H_R+N)_{t=D_p}}{(H_L+H_R+N)_{t=0}}$
Average copies of viral DNA per cell [23, 27]	n_T	50-70	-	$n_T = \left(\frac{L+R+V_I}{H_L+H_R+N}\right)_{t\to\infty}$
Average number of lytic DNA per cell	R_A	-	-	$\left(\frac{R}{H_R}\right)_{t\to\infty}$
Average number of intracellular DNA per cell	V_{IA}	-	-	$\left(\frac{V_I}{H_R}\right)_{t\to\infty}$

Table 2: Observed cell line constants.

From the constants and relationships in Table 2, the uninduced equations (3.3), and the above estimates for q, d_R, γ_R, and $d_I(\bar{V}_I) = c\bar{V}_I$, we obtain the following parameter values in terms of the unknown parameters γ_L, μ,

$$\begin{aligned} d_L &= \frac{\ln(2)/D_p + \mu N_r}{1 - a_s - N_r} - \gamma_L \\ c &= \frac{\ln(2)}{a_s V_{IA} D_p}(N_r - 1) + \frac{\gamma_L}{a_s V_{IA}}(1 - a_s - N_r) \\ \alpha_0 &= \gamma_L - \frac{\ln(2)}{D_p} \\ p &= \frac{R_A}{T V_{IA}} - \frac{(1 - a_s - N_r)}{a_s}\left(\gamma_L - \frac{\ln(2)}{D_p}\right) \\ \kappa &= \left(\frac{\gamma_L - \ln(2)/D_p}{a_s R_A}\right)(R_A - N_r R_A - n_T + a_s V_{IA}) + \frac{1}{T} \\ n &= \frac{n_T - a_s(R_A + V_{IA})}{1 - a_s - N_r}\,. \end{aligned} \tag{5.7}$$

6 Numerical Results

In this section, we compare our reactivation model to two sets of experimental data from the literature that describe reactivation of latent virus in BCBL-1 cells. In particular, we compare our model to longitudinal cell viability data following chemical induction. In one case, Zoeteweij, *et al.*, [38] use *n*-butyric acid ($CH_3CH_2CH_2COOH$) as the inducing agent, while in the other case, Yu, *et al.*, [37] use Na *n*-butyrate ($CH_3CH_2CH_2COONa$) as the inducing agent. Despite the differences in molecular formulas, we expect the two inducers to behave roughly the same in solution after dissociation of the H^+ and Na^+ ions. In particular, for cell viability data, Sakurazawa, *et al.*, have shown that *n*-butyric acid and Na *n*-butyrate are cytotoxic at approximately the same concentrations [31].

6.1 Parameter values

In Section 5 we estimated values for some parameters from physiological considerations and showed that other model parameters could be estimated from a few free parameters and experimental observations of cell-line constants (5.7). The fraction of nonviable cells N_r (in the uninduced case) is the only value that we can determine directly from the data of Zoeteweij, *et al.*, and Yu, *et al.*, obtaining approximate values of 8% and 17%, respectively. For the other constants we choose values from within the ranges reported in the literature (Table 2): $a_s = 0.017$, $Dp = 85$ hr. In addition, we choose $n_T = 70$ and 63 for modeling the data of Zoeteweij, *et al.*, and Yu, *et al.*., respectively. In this way we have $n = 74$ for both sets of data. We choose the following values for the free parameters and unknown constants : $\gamma_L = 8.4 \times 10^{-3}$ hr^{-1}, $\mu = 2.1 \times 10^{-4}$ hr^{-1}, $R_A = 89$, and $V_{IA} = 89$.

In Table 3 we tabulate the parameter values used in simulations corresponding to the above choices of experimental constants and free parameters.

Parameter	Symbol	Zoeteweij, *et al.*, data	Yu, *et al.*, data	Units
Net growth rate constants for host cells	γ_L	8.4×10^{-3}	8.4×10^{-3}	hr^{-1}
	γ_R	0	0	hr^{-1}
Natural death rate constant for host cells	d_L	6.49×10^{-4}	1.70×10^{-4}	hr^{-1}
	d_R	0	0	hr^{-1}
Spontaneous reactivation rate constant for latently infected host cells	α_0	2.45×10^{-4}	2.45×10^{-4}	hr^{-1}
Spontaneous deactivation rate constant for lytically infected host cells	ρ	0	0	hr^{-1}
Rate constant for cell death due to viral lysis	c	5.48×10^{-5}	3.99×10^{-5}	hr^{-1}
Rate constant for nonviable cell degradation	μ	2.1×10^{-4}	2.1×10^{-4}	hr^{-1}
Rate constant for synthesis of viral DNA	κ	2.30×10^{-2}	2.28×10^{-2}	hr^{-1}
Rate constant for sequestration of viral DNA for encapsulation	q	2.08×10^{-2}	2.08×10^{-2}	hr^{-1}
Rate constant for packaging and secretion of virions	p	7.80×10^{-3}	9.13×10^{-3}	hr^{-1}
Average number of copies of viral DNA per latent host cells	n	74	74	-
Induced reactivation rate constant	α_c	8.72×10^{-1}	1.85×10^{-1}	hr^{-1}
Induced death rate constant	δ_c	5.33×10^{-3}	6.91×10^{-3}	hr^{-1}
Induced death rate	$\delta_L(s)$	0	0	hr^{-1}

Table 3: Parameters from the uninduced model (3.3) are calculated from (5.7) with constants $a_s = 0.017$, $V_{IA} = 89$, $R_A = 89$, $N_r = 0.08$ or 0.17, $D_p = 85$ hr, and $n_T = 70$ or 63, and with free parameters $\gamma_L = 8.4 \times 10^{-3}$ hr^{-1} and $\mu = 2.1 \times 10^{-4}$ hr^{-1}. Parameters from the induced model (4.5) are obtained from fits to experimental data.

6.2 Uninduced Case

We first present results of a simulation for the uninduced case modeled by system (3.3). Parameter values used for the simulation are shown in Table 3. The initial condition for all compartments is zero, except for compartments H_L and L, which have initial conditions of 1.0×10^6 and 7.4×10^7. Figure 2 depicts the fraction of nonviable cells $N/(H_L + H_R + N)$ (dashed lines) and the fraction of spontaneously reactivated cells $H_R/(H_L + H_R + N)$ from simulations using equations (3.3) and the parameter values in Table 3. In Fig. 2 we can see that, by 1000 hours, the fraction of nonviable cells and the fraction of spontaneously reactivated cells asymptotically reach the specified equilibrium values of $a_s = 0.017$ and $N_r = 0.08$ for the data of Zoeteweij, *et al.*, and $a_s = 0.017$ and $N_r = 0.17$ for the data of Yu, *et al.* By equilibrium we mean that, although the cell culture is growing exponentially, certain characteristic properties related to the ratios

of model compartments eventually become constants (see Table 2).

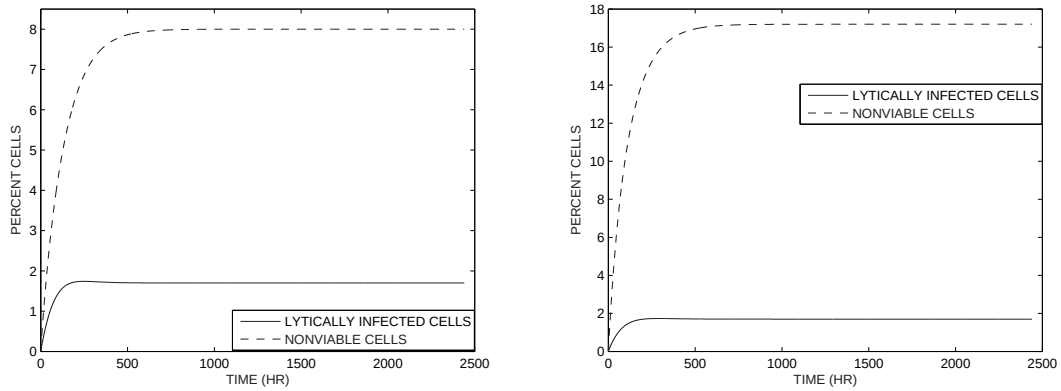

(a) (b)

Figure 2: Uninduced simulations using equations (3.3) and parameters from Table 3 for the data of a) Zoeteweij, *et al.*, and b) Yu, *et al.* Solid lines plot the percentage of cells that are spontaneously reactivated $H_R/(H_L + H_R + N)$, while dashed lines plot the percentage of cells that are nonviable cells $N/(H_L + H_R + N)$.

In Fig. 3 we can see a similar equilibration of the average number of lytic and intracellular DNA copies per lytically infected host cell, R/H_R and V_I/H_R, respectively. In Fig. 3 we can see that, by 1000 hours, the quantities R/H_R an V_I/H_R have reach the specified equilibrium values of $R_A = 89$ and $V_{IA} = 89$, respectively (see Table 2).

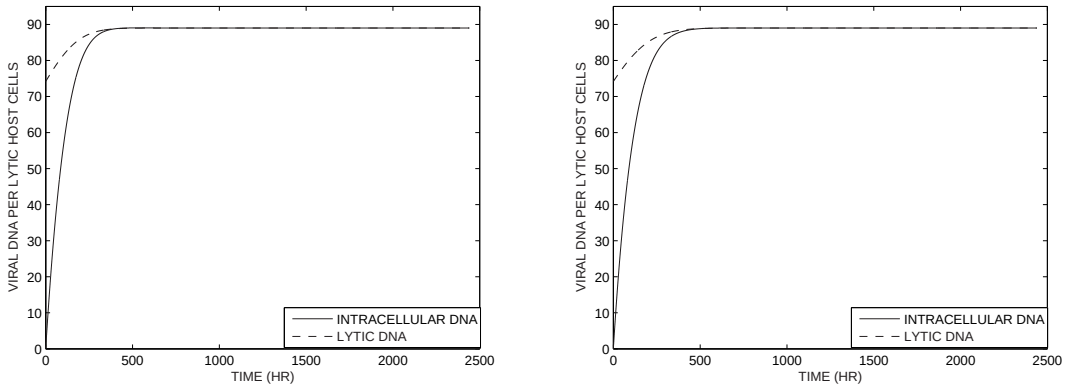

(a) (b)

Figure 3: Uninduced simulations using equations (3.3) and parameters from Table 3 for the data of a) Zoeteweij, *et al.*, and b) Yu, *et al.* The plots show the average number of lytic viral DNA copies R/H_R (dashed line) and the average number of intracellular viral DNA copies V_I/H_R (solid line) per lytically infected host cell. Both quantities start with an initial condition of zero, but the quantity R/H_R grows quite rapidly, giving the appearance of having a nonzero starting value for these plot limits.

The equilibrated simulations for the uninduced model approximate the properties of the uninduced cell cultures that are subsequently used in induction experiments and provide initial conditions for simulation of the induced equations (4.5).

6.3 Induced Case

Next we report on simulations for the induced equations (4.5). In the case of those parameters that are common to both the uninduced and induced models we use the same values as in the previous simulation (Table 3). Initial conditions for the induced model are obtained from the simulations of the uninduced model at $t = 2400$ hr. Not only is the inducing agent capable of reactivating the latent virus, but it can also activate host cell genes that may lead to apoptosis. We make a simplifying assumption that activation of host cell genes would most likely occur in conjunction with reactivation of latent virus. In other words, we assume that inducing mechanisms that would initiate cell apoptosis would also lead to viral reactivation and, therefore, assume that there will be no chemically induced cell death for latently infected host cells (i.e., $\delta_L = 0$).

The exact functional forms of the rates for induced lytic cell death $\delta_R(s)$ and induced reactivation of latent cells $\alpha(s)$ are not known. We first choose simple affine functions $\alpha(s) = \alpha_0 + \alpha_c s$ and $\delta_R(s) = \delta_c s$ and find values for the function parameters by fitting longitudinal experimental data on BCBL-1 cell viability from Zoeteweij, *et al.*, [38] and Yu, *et al.*, [37], separately. The parameter fitting is accomplished by forming an ordinary least squares inverse problem as described in the Appendix and then estimating the parameters using a Nelder-Mead algorithm. Standard errors are calculated, the details of which are also given in the Appendix. In the case of the affine functions, estimated values for the parameters are insensitive to the initial values that seed the optimization algorithm.

Figure 4 compares cell viability predicted from simulations with data from both experimental groups, using the estimated parameters for δ_c and α_c obtained by the ordinary least squares estimation techniques. Estimated parameter values are reported in Table 3 and 4. Some of the model parameters differ between the two groups because of differences in uninduced cell viability for the two groups (92% versus 83%). From Fig. 4 it can be seen that the simulations for the induced model qualitatively match the behavior of the experimental data.

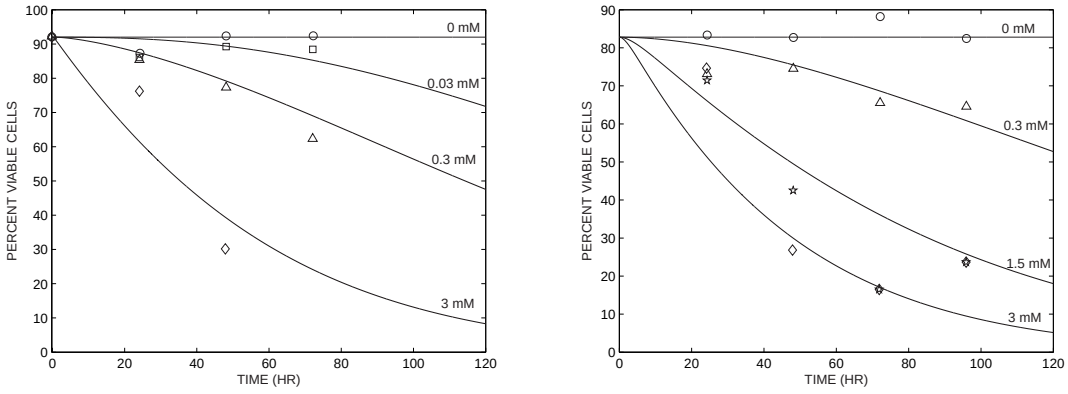

(a) (b)

Figure 4: Comparison of cell viability measurements with simulations using induced equations (4.5) and fitted parameters for linear functions $\alpha(s)$ and $\delta_R(s)$: a) Zoeteweij, *et al.*, circles 0 mM, squares 0.03 mM, triangles 0.3 mM, and diamonds 3 mM, $\alpha_c = 0.872$, $\delta_c = 5.33 \times 10^{-3}$ and b) Yu, *et al.*, circles 0 mM, triangles 0.3 mM, stars 1.5 mM, and diamonds 3 mM, $\alpha_c = 0.185$, $\delta_c = 6.91 \times 10^{-3}$.

In Fig. 5 we plot the number of free virions as a function of time for different butyrate concentrations. Yu, *et al.*, [37] observe in their experiments that high concentrations of butyrate (1.5 and 3 mM) greatly increase lytic activity, but also significantly increase cell death. The end result is that, even after 5 days, very few free virions are produced because of massive amounts of cell death before the end of the lytic program. This is contrasted by observations at smaller concentrations of butyrate (≤ 0.3 mM), where much less cell death is seen and there is significant secretion of free virions. In Fig. 5 it can be seen that there is approximately a three-fold increase in free virion produced at 0.3 mM concentration of butyrate as compared to the 3 mM concentration.

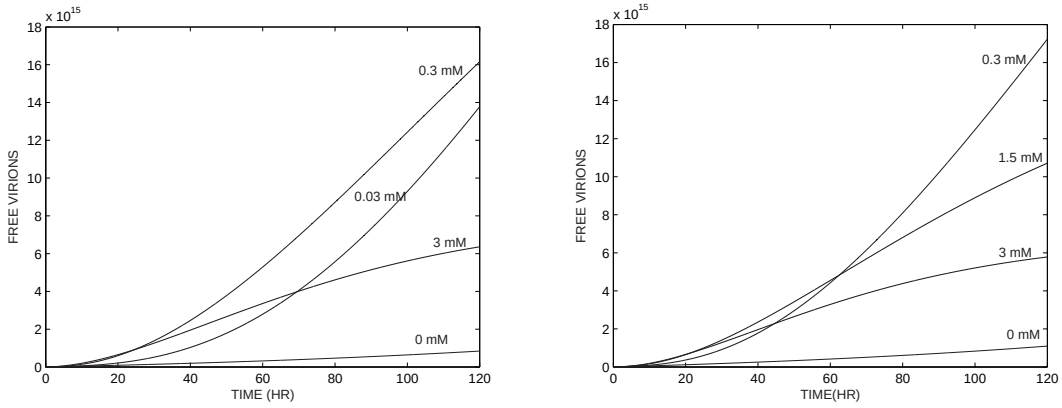

(a) (b)

Figure 5: The results of simulations of free virions produced using induced equations (4.5) and parameters for linear functions $\alpha(s)$ and $\delta_R(s)$ fitted to experimental data from a) Zoeteweij, *et al.*, and b) Yu, *et al.*

Table 4 summarizes the estimated parameters, standard errors, and confidence intervals obtained from fitting the induced equations (4.5) with the parameter functions $\alpha(s) = \alpha_0 + \alpha_c s$ and $\delta_R(s) = \delta_c s$ to both sets of data. Table 4 shows that the estimated parameter values for both groups are within an order of magnitude of each other. Differences between the parameter values may reflect differences in the cell growth and maintenance conditions or differences in experimental measurement techniques. Even in the uninduced case, there is a difference in the cell viability for both groups, with $N_r = 0.08$ for the data of Zoeteweij, *et al.*, and $N_r = 0.17$ for the data of Yu, *et al.* In addition, Zoeteweij, *et al.*, measure cell viability using Dead Red staining and flow cytometry, while Yu, *et al.*, measure cell viability with trypan blue staining and counting on a haemocytometer. In Table 4, it can also be seen that the standard errors for the reactivation rate constants α_c are at least an order of magnitude less than the parameter values. However, the standard errors for the induced death rate constants δ_c are the same order of magnitude as the parameter values, providing us with less confidence in values obtained for δ_c.

Data	Parameter	Estimated Value	Standard Error	Confidence Interval
Zoeteweij, *et al.*	δ_c	5.33×10^{-3}	3.91×10^{-3}	$[-3.11 \times 10^{-3}, 1.38 \times 10^{-2}]$
	α_c	8.72×10^{-1}	1.26×10^{-2}	$[8.45 \times 10^{-1}, 8.99 \times 10^{-1}]$
Yu, *et al.*	δ_c	6.91×10^{-3}	3.70×10^{-3}	$[-1.03 \times 10^{-3}, 1.48 \times 10^{-2}]$
	α_c	1.85×10^{-1}	1.11×10^{-2}	$[1.61 \times 10^{-1}, 2.09 \times 10^{-1}]$

Table 4: Estimated parameter values, standard errors, and confidence intervals

7 Discussion

In other simulations, we used different functional forms for $\alpha(s)$ and $\delta_R(s)$, including Michaelis-Menton and sigmoid functions, but we found that the fits of the induced equations to cell viability data were relatively insensitive to more complicated functional forms (data not shown) and that reasonable fits to cell viability data were obtained by assuming simple linear functions. However, with more data, especially with data for viral DNA compartments, we expect to be able to determine optimal functional forms for $\alpha(s)$ and $\delta_R(s)$, for example, combinations of linear, Michaelis-Menton, and sigmoid functions. Alternatively, instead of fixing the functional form of $\alpha(s)$ and $\delta_R(s)$ a priori in parametric form, we could estimate the shape of the functional form itself using approximation by piece-wise linear splines or other approximations as has been successfully done in other problems in, for example, [1, 3].

Even though this preliminary model yields good qualitative agreement with cell viability data, additional experimental data is needed to compare model predictions to other measurable quantities of interest, such as cell-associated DNA ($L + R + V_I$) and free virions (V_F). Additional data would also help to determine the free parameters γ_L and μ, as well as the unknown constants R_A and V_{IA}. In the case of R_A and V_{IA}, parameter sensitivity tests show that the optimal parameter values δ_c and α_c are relatively insensitive to variations in R_A or V_{IA}, since varying R_A or V_{IA} by $\pm$ 5% produced 3% or less variation in the optimized parameter values.

Instead of a single viral compartment R to quantify copies of viral DNA in the lytic program, we could modify the model to describe Immediate Early, Early, and Late gene expression (RNA), represented by

compartments R_1, R_2, and R_3 in the following equations for an induced model

$$\begin{aligned}
\frac{dH_L}{dt} &= (\gamma_L - \alpha(s) - \delta_L(s))\, H_L + \rho H_R \\
\frac{dH_R}{dt} &= \left(\gamma_R - \delta_R(s) - d_I(\bar{V}_I) - \rho\right) H_R + \alpha(s) H_L \\
\frac{dN}{dt} &= \left(d_L + \delta_L(s)\right) H_L + \left(d_R + \delta_R(s) + d_I(\bar{V}_I)\right) H_R - \mu N \\
\frac{dL}{dt} &= (\gamma_L - \alpha(s) - \delta_L(s))\, L + \rho(R_1 + R_2 + R_3) \\
\frac{dR_1}{dt} &= \left(\gamma_R - q_1 - \delta_R(s) - d_I(\bar{V}_I) - \rho\right) R_1 + \alpha(s) L \\
\frac{dR_2}{dt} &= \left(\kappa + \gamma_R - q_2 - \delta_R(s) - d_I(\bar{V}_I) - \rho\right) R_2 + q_1 R_1 \\
\frac{dR_3}{dt} &= \left(\gamma_R - q - \delta_R(s) - d_I(\bar{V}_I) - \rho\right) R_3 + q_2 R_2 \\
\frac{dV_I}{dt} &= q R_3 - \left(p + d_R + d_I(\bar{V}_I) + \delta_R(s)\right) V_I
\end{aligned} \tag{7.8}$$

and $V_F(t) = V_{F0} + \int_{t_0}^{t} p V_I(u) du$.

The three parameters q_1, q_2, and q_3 represent the rate at which viral DNA moves from one stage of the lytic program to the next. These parameters can be estimated as $1/T_1$, $1/T_2$, and $1/T_3$, respectively, where T_1, T_2, and T_3 are the approximate times for each stage of the lytic program. Corresponding parameters in this proposed model and (4.5) would not necessarily represent the same quantities.

By having model compartments that quantify RNA production or promoter activity from genes representative of each stage of the lytic cycle, we can hope to predict viral reactivation in more detail and compare to experimental gene expression data. For example, ORF50, vIL6, K8.1 could be representative of the Immediate Early, Early, and Late stages, respectively. A single compartment L can represent latent gene expression, primarily ORF73 expression.

There may be underlying biological delays, due to the ordered cascade of gene expression that makes up the lytic program, that are not captured with the model (4.5). A model such as (7.8) in which we rewrite the single R compartment as three compartments R_1, R_2, and R_3 representing the Immediate Early, Early, and Late phases of the lytic program might be expected to more closely capture the biological delays inherent in the lytic program of system.

8 Conclusion

We have developed a preliminary deterministic mathematical model to describe reactivation of latent virus by chemical inducers. In particular, we apply this model to the reactivation of latent KSHV in BCBL-1 cell cultures with butyrate as the inducing agent. We first estimate parameters for our uninduced model from physiological considerations and known properties of these exponentially growing, uninduced cell cultures. We then extend the model to describe chemically induced KSHV reactivation in latently infected BCBL-1 cells. Additional parameters that describe induction are determined from fits to experimental data available in the literature. Our model provides good agreement with two independent sets of experimental data. While this preliminary model yields good qualitative agreement with cell viability data for KSHV induced

by butyrate, it also strongly suggests the need for further experiments designed explicitly to support model development and validation in providing not only more but also additional types of longitudinal data.

This model exploits the polymicrobial nature of reactivation by focusing on chemical inducers that utilize the same mechanisms as gram negative anaerobic bacteria. Among viruses there can be interactions that result in reactivation as well. For example, recent experiments have shown that KSHV enhances HIV replication and reactivation [9, 11] and that KSHV ORF50 (lytic) gene products increase in vitro cell susceptibility to human immunodeficiency virus type 1 infection [10]. This evidence for the synergistic interactions of KSHV and HIV highlights the importance of further model development and application to polymicrobial environments.

Application of the type of model we have developed here to other latent viruses could provide information about the similarities and differences among latent virus systems and could define the relationship of these organisms to their inducers. For example, like KSHV, many latent viruses are induced to replication via HDAC inhibition and are responsive to agents like sodium butyrate. These include EBV, HCMV, HSV, HIV, Adenovirus, HPV, and HTLV1. The model with appropriate variations could potentially be applied to any of these viruses. Further, the use of this and future models with other inducers may also provide extremely valuable clinical information about induction mechanisms.

9 Appendix

In this appendix we discuss the asymptotic theory used to compute the standard errors and confidence intervals in Table 4 of Section 6.3. We first give a general summary of the theory.

We assume N^* scalar longitudinal/inducer level observations (time/inducer series of numbers or ratios of numbers of cells as described below) are represented by the statistical model

$$Y_j \equiv f_j(\theta_0) + \epsilon_j, \;\; j = 1, 2, \ldots N^*, \tag{9.9}$$

where $f_j(\theta_0)$ is the model for the observations in terms of the state variables and $\theta_0 \in \mathbb{R}^m$ is a "set" of theoretical "true" parameter values (assumed to exist in a standard statistical approach). We assume for our statistical model of the observation or measurement process (9.9) that the errors ϵ_j, $j = 1, 2, \ldots, N^*$, are independent identically distributed (*i.i.d.*) random variables with mean $E[\epsilon_j] = 0$ and constant variance $var[\epsilon_j] = \sigma_0^2$, where of course σ_0^2 is unknown (standard residual plots with the data used in our simulation suggested this assumption of constant variance). We then have that the observations Y_j are *i.i.d.* with mean $E[Y_j] = f_j(\theta_0)$ and variance $var[Y_j] = \sigma_0^2$.

We consider estimation of parameters using an ordinary least squares (OLS) approach. Thus we seek to use data $\{y_j\}$ for the observation process $\{Y_j\}$ with the model to seek a value $\hat{\theta}$ that minimizes

$$J(\theta) = \sum_{j=1}^{N^*} |y_j - f_j(\theta)|^2. \tag{9.10}$$

Since Y_j is a random variable, we have that the estimator $\hat{\theta}_{OLS}$ is also a random variable with a distribution called the *sampling distribution*. Knowledge of this sampling distribution provides uncertainty information (e.g., standard errors) for the numerical values of $\hat{\theta}$ obtained using a specific data set $\{y_j\}$ (i.e., a realization of $\{Y_j\}$) when minimizing $J(\theta)$.

Under reasonable assumptions on smoothness and regularity (the smoothness requirements for model solutions are readily verified using continuous dependence results for ordinary differential equations in our example; the regularity requirements involve, among others, conditions on how the observations are taken as sample size increases, i.e., $N^* \to \infty$), the standard nonlinear regression approximation theory ([15], [19], [21], and Chapter 12 of [32]) for asymptotic (as $N^* \to \infty$) distributions can be invoked. This theory yields that

the sampling distribution $\hat{\theta}(Y)$ for the estimate $\hat{\theta}$, where $Y = \{Y_j\}_{j=1}^{N^*}$, is approximately a m-multivariate Gaussian with mean $E[\hat{\theta}(Y)]$ and covariance matrix $cov[\hat{\theta}(Y)] = \Sigma_0 = \sigma_0^2[\chi^T(\theta_0)\chi(\theta_0)]^{-1}$. Here $\chi(\hat{\theta}) = F_\theta(\theta)$ is the $N^* \times m$ sensitivity matrix with elements

$$\chi_{jk}(\theta) = \frac{\partial f_j(\theta)}{\partial \theta_k} \qquad \text{and} \qquad F_\theta(\theta) \equiv (f_{1\theta}(\theta), \ldots, f_{N^*\theta}(\theta))^T.$$

That is, for N^* large, the sampling distribution approximately satisfies

$$\hat{\theta}_{OLS}(Y) \sim \mathcal{N}_m(\theta_0, \sigma_0^2[\chi^T(\theta_0)\chi(\theta_0)]^{-1}) := \mathcal{N}_m(\theta_0, \Sigma_0). \tag{9.11}$$

The elements of the matrix $\chi = (\chi_{jk})$ can be estimated using the forward difference

$$\chi_{jk}(\theta) = \frac{\partial f_j(\theta)}{\partial \theta_k} \approx \frac{f_j(\theta + h_k) - f_j(\theta)}{h_k},$$

where h_k is an m-vector with nonzero entry in only the k^{th} component, or using sensitivity equations (see [4] and the references therein). For our efforts here we chose the sensitivity equation approach as explained below. Since θ_0, σ_0 are not known, we must approximate them in $\Sigma_0 = \sigma_0^2[\chi^T(\theta_0)\chi(\theta_0)]^{-1}$. For this we follow standard practice and use the approximation

$$\Sigma_0 \approx \Sigma(\hat{\theta}) = \hat{\sigma}^2[\chi^T(\hat{\theta})\chi(\hat{\theta})]^{-1}$$

where $\hat{\theta}$ is the parameter estimate obtained, and the approximation $\hat{\sigma}^2$ to σ_0^2 is given by

$$\sigma_0^2 \approx \hat{\sigma}^2 = \frac{1}{N^* - m} \sum_{j=1}^{N^*} |y_j - f_j(\hat{\theta})|^2.$$

Standard errors to be used in confidence interval calculations are thus given by $SE_k(\hat{\theta}) = \sqrt{\Sigma_{kk}(\hat{\theta})}$, $k = 1, 2, \ldots, m$ (see [12]).

In the induced case example of Section 6.3, we consider the parametric functional forms $\delta_R(s) = d_c s$ and $\alpha(s) = \alpha_c s + \alpha_0$. If we let $x = (H_L, H_R, N, L, R, V_I, V_F)^T$ and denote $\theta = (\delta_c, \alpha_c)$, then the differential equations in the induced case can be written in a general form

$$\begin{aligned} \dot{x} &= g(t, x, s, \theta) \\ x(0) &= x_0, \end{aligned} \tag{9.12}$$

where $g : \mathbb{R}_+ \times \mathbb{R}^{n^*} \times \mathbb{R}_+ \times \mathbb{R}^m \to \mathbb{R}^{n^*}$ for $n^* = 7$, $m = 2$, and $x_0 = (H_{L0}, H_{R0}, N_0, L_0, R_0, V_{I0}, V_{F0})^T$. Since the experimental data are given in percentage of viable cells, we define the outputs of the model

$$f(t, s, \theta) = \left[\frac{V_{total}(t, s, \theta) - N(t, s, \theta)}{V_{total}(t, s, \theta)} \right], \qquad t, s \geq 0,$$

where $V_{total} = H_L + H_R + N$. In each parameter fit, we use data that is longitudinal (taken at t_k) and across several levels s_i of inducer. This is indexed by $\tau_j = (t_k, s_i)$ for $k = 1, \ldots, K$, $i = 1, \ldots, I$, and observations y_j for the model values $f_j(\theta) = f(t_k, s_i, \theta), j = 1, \ldots, N^* = KI$. Then, we construct the OLS estimator by minimizing the cost criterion (9.10) where $\{y_j\}$ denotes the experimental data (in the data of Section 6.3 we had $N^* = 15$ or 16 resulting from $K = 4$ and $I = 4$ – see Figure 4). For the optimization in θ we used the Nelder-Mead algorithm.

To compute the covariance matrix Σ we need the sensitivity matrix F_θ. That is, $\chi(\hat{\theta}) = \dfrac{\partial F}{\partial \theta}(\hat{\theta})$. From the outputs defined in (9.12), it suffices to have the sensitivities $\dfrac{\partial x}{\partial \theta}$. To compute these we used the sensitivity equation method which involves solving the $n^* \times m$ matrix *variational differential equation*

$$\frac{d}{dt}\left(\frac{\partial x}{\partial \theta}\right) = \frac{\partial g}{\partial x}\frac{\partial x}{\partial \theta} + \frac{\partial g}{\partial \theta}, \tag{9.13}$$

where the matrix coefficient and the forcing function in this equation are evaluated along solutions of the system equation (9.12). Note that this variational equation can be solved simultaneously (see [4] for details) with the system equation (9.12).

Finally, in order to compute the confidence intervals (at the $100(1-c)\%$ level) for the estimated parameters in our example, we define the confidence level parameters associated with the estimated parameters so that

$$P(\hat{\theta}_k - t_{c/2} SE_k(\hat{\theta}) < \theta_k < \hat{\theta}_k + t_{c/2} SE_k(\hat{\theta})) = 1 - c, \tag{9.14}$$

where $c \in [0,1]$, and $t_{c/2} \in \mathbb{R}_+$. For a given c value (small, say $c = .05$ for 95% confidence intervals), the critical value $t_{c/2}$ is computed from the Student's t distribution t^{N^*-m} with $N^* - m$ degrees of freedom since for each of the data sets available to us we have N^* is less than 30. The value of $t_{c/2}$ is determined by $P(T \geq t_{c/2}) = c/2$ where $T \sim t^{N^*-m}$.

10 Acknowledgements

This research was supported in part by the US Air Force Office of Scientific Research under grant AFOSR FA9550-04-1-0220, in part by the Joint DMS/NIGMS Initiative to Support Research in the Area of Mathematical Biology under grant 1R01GM67299-01, in part by the National Science Foundation under grant DMS-0112069 to the Statistical and Applied Mathematical Sciences Institute (SAMSI), and in part by the UNC Center for AIDS Research under grant K23 DE 00460-01.

References

[1] Adams, BM, *Non-parametric Parameter Estimation and Clinical Data Fitting With a Model of HIV Infection*, Ph.D. Thesis, Center for Research in Scientific Computation, Mathematics Department, North Carolina State University, 2005.

[2] Banks HT, Bortz DM, and Holte SE, Incorporation of variability into the mathematical modeling of viral delays in HIV infection dynamics, *Mathematical Biosciences* **183**, 63–91, 2003.

[3] Banks HT, and Kunisch K, *Estimation Techniques for Distributed Parameter Systems*, Birkhaüser, Boston, 1989.

[4] Banks HT, and Nguyen HK, Sensitivity of dynamical system to Banach space parameters, CRSC Tech Rep., CRSC-TR05-13, N.C. State University, Feb., 2005; *J. Math Anal. Appl.*, to appear.

[5] Bechtel JT, Liang YY, Hvidding J, et al., Host range of Kaposi's sarcoma-associated herpesvirus in cultured cells, *Journal of Virology* **77** (11), 6474-6481, 2003.

[6] Bernhard D, Ausserlechner MJ, Tonko M, et al., Apoptosis induced by the histone deacetylase inhibitor sodium butyrate in human leukemic lymphoblasts, *FASEB Journal* **13** (14), 1991-2001, 1999.

[7] Blower SM, Porco TC, and Darby G, Predicting and preventing the emergence of antiviral drug resistance in HSV-2, *Nature Medicine* **4** (6), 673-678, 1998.

[8] Cannon JS, Ciufo D, Hawkins AL, et al., A new primary effusion lymphoma-derived cell line yields a highly infectious Kaposi's sarcoma herpesvirus-containing supernatant, *Journal of Virology* **74** (21), 10187-10193, 2000.

[9] Caselli E, Menegazzi P, Bracci A, Galvan M, Cassai E, and Di Luca D, Human herpesvirus-8 (Kaposis sarcoma-associated herpesvirus) ORF50 interacts synergistically with the tat gene product in transactivating the human immunodeficiency virus type 1 LTR, *J Gen Virol.,* **82**, 1965-1970, 2001.

[10] Caselli E, Galvan M, Santoni F, et al., Human herpesvirus- 8 (Kaposis sarcoma-associated virus) ORF50 increases in vitro cell susceptibility to human immunodeficiency virus type 1 infection, *J Gen Virol.,* **84**, 1123-1131, 2003.

[11] Caselli E, Galvan M, Cassai E, et al., Human herpesvirus 8 enhances human immunodeficiency virus replication in acutely infected cells and induces reactivation in latently infected cells, *Blood* **106**, 2790-2797, 2005

[12] Casella G, and Berger RL, *Statistical Inference*, Duxbury, California, 2002.

[13] Chan SR, Bloomer C, and Chandran B, Identification and characterization of human herpesvirus-8 lytic cycle-associated ORF59 protein and the encoding cDNA by monoclonal antibody, *Virology* **240** (1), 118-126, 1998.

[14] Csordas A, Toxicology of butyrate and short-chain fatty acids, in *Role of Gut Bacteria in Human Toxicology and Pharmacology*, M.J. Hill, Editor, Taylor & Francis, London, 1995.

[15] Davidian M, and Giltinan DM, *Nonlinear Models for Repeated Measurement Data*, Chapman and Hall/ CRC, Boca Raton, 1995.

[16] Flint SJ, Enquist LW, Racaniello VR, and Skalka AM, *Principles of Virology*, ASM Press, Washington DC, 2004.

[17] Friborg J, Kong WP, Hottiger MO, et al., p53 inhibition by the LANA protein of KSHV protects against cell death, *Nature* **402** (6764), 889-894, 1999.

[18] Garnett GP, Grenfell BT, The epidemiology of varicella zoster virus-infections - a mathematical-model, *Epidemiology and Infection* **108** (3), 495-511, 1992.

[19] Gallant AR, *Nonlinear Statistical Models*, John Wiley & Sons, Inc., New York, 1987.

[20] Izumiya Y, Lin SF, Ellison TJ, et al., Cell cycle regulation by Kaposi's sarcoma-associated herpesvirus K-bZIP: Direct interaction with cyclin-CDK2 and induction of G(1) growth arrest, *Journal of Virology* **77** (17), 9652-9661, 2003.

[21] Jennrich RI, Asymptotic properties of non-linear least squares estimators, *Ann. Math. Statist.*, **40**, 633–643, 1969.

[22] Klass CM, Krug LT, Pozharskaya VP, et al., The targeting of primary effusion lymphoma cells for apoptosi by inducing lytic replication of human herpesvirus 8 while blocking virus production, *Blood* **105** (10), 4028-4034, 2005.

[23] Lallemand F, Desire N, Rozenbaum M, *et al.*, Quantitative analysis of human herpesvirus 8 viral load using real-time PCR assay, *Journal of Clinical Microbiology* **38** (4), 1404-1408, 2000.

[24] Lu M, Suen J, Frias C, et al., Dissection of the Kaposi's sarcoma-associated herpesvirus gene expression program by using the viral DNA replication inhibitor cidofovir, *Journal of Virology* **78** (24), 13637-13652, 2004.

[25] Lukac DM, Kirshner JR, and Ganem D, Transcriptional activation by the product of open reading frame 50 of Kaposi's sarcoma-associated herpesvirus is required for lytic viral reactivation in B cells, *Journal of Virology* **73** (11), 9348-9361, 1999.

[26] Lukac DM, Renne R, Kirshner JR, et al., Reactivation of Kaposi's sarcoma-associated herpesvirus infection from latency by expression of the ORF50 transactivator, a homolog of the EBV R protein, *Virology* **252** (2), 304-312, 1998.

[27] Renne R, Lagunoff M, Zhong WD, et al., The size and conformation of Kaposi's sarcoma-associated herpesvirus (human herpesvirus 8) DNA in infected cells and virions, *Journal of Virology* **70** (11), 8151-8154, 1996.

[28] Renne R, Zhong WD, Herndier B, et al., Lytic growth of Kaposi's sarcoma-associated herpesvirus (human herpesvirus 8) in culture, *Nature Medicine* **2** (3), 342-346, 1996.

[29] Rothwell R, Morris T, Granger D, Dominick L, Picot B, Duus K, and Webster-Cyriaque J., Pathogenic aneaorobic bacteria cause epigenetic changes that result in viral reactivation, submitted.

[30] Said JW, Chien K, Tasaka T, et al., Ultrastructural characterization of human herpesvirus 8 (Kaposi's sarcoma-associated herpesvirus) in Kaposi's sarcoma lesions: Electron microscopy permits distinction from cytomegalovirus (CMV), *Journal of Pathology* **182** (3), 273-281, 1997.

[31] Sakurazawa T, and Ohkusa T, Cytotoxicity of organic acids produced by anaerobic intestinal bacteria on cultured epithelial cells, *Journal of Gastroenterology* **40** (6), 600-609, 2005.

[32] Seber GAF and Wild CJ, *Nonlinear Regression*, John Wiley & Sons, Inc., New York, 1989.

[33] Tinari A, Monini P, Marchetti M, *et al.*, Lytic growth of human herpesvirus 8: Morphological aspects, *Ultrastructural Pathology* **24**, 301-310, 2000.

[34] Wang GY, Krueger GRF, and Buja LM, Mathematical model to simulate the cellular dynamics of infection with human herpesvirus-6 in EBV-negative infectious mononucleosis, *Journal of Medical Virology* **71** (4), 569-577, 2003.

[35] Wu FY, Ahn JH, Alcendor DJ, et al., Origin-independent assembly of Kaposi's sarcoma-associated herpesvirus DNA replication compartments in transient cotransfection assays and association with the ORF-K8 protein and cellular PML, *Journal of Virology* **75** (3), 1487-1506, 2001.

[36] Wu FY, Tang QQ, Chen HL, et al., Lytic replication-associated protein (RAP) encoded by Kaposi sarcoma-associated herpesvirus causes p21(CIP-1)-mediated G(1) cell cycle arrest through CCAAT/enhancer-binding protein-alpha, *Proceedings of the National Academy of Sciences USA* **99** (16), 10683-10688, 2002.

[37] Yu Y, Black JB, Goldsmith CS, *et al.*, Induction of human herpesvirus-8 DNA replication and transcription by butyrate and TPA in BCBL-1 cells, *Journal of Virology* **80**, 83-90, 1999.

[38] Zoeteweij JP, Eyes ST, Orenstein JM, et al., Identification and rapid quantification of early- and late-lytic human herpesvirus 8 infection in single cells by flow cytometric analysis: Characterization of antiherpesvirus agents, *Journal of Virology* **73** (7), 5894-5902, 1999.